



HAL
open science

Electronically Re-Configurable, Non-Volatile, Nano-Ionics-Based RF-Switch on Paper Substrate for Chipless RFID Applications

Jayakrishnan Methapettyparambu Purushothama, Arnaud Vena, Brice Sorli,
Etienne Perret

► **To cite this version:**

Jayakrishnan Methapettyparambu Purushothama, Arnaud Vena, Brice Sorli, Etienne Perret. Electronically Re-Configurable, Non-Volatile, Nano-Ionics-Based RF-Switch on Paper Substrate for Chipless RFID Applications. *Technologies*, 2018, 6 (3), pp.58. 10.3390/technologies6030058. hal-01992062

HAL Id: hal-01992062

<https://hal.science/hal-01992062>

Submitted on 13 Jan 2020

HAL is a multi-disciplinary open access archive for the deposit and dissemination of scientific research documents, whether they are published or not. The documents may come from teaching and research institutions in France or abroad, or from public or private research centers.

L'archive ouverte pluridisciplinaire **HAL**, est destinée au dépôt et à la diffusion de documents scientifiques de niveau recherche, publiés ou non, émanant des établissements d'enseignement et de recherche français ou étrangers, des laboratoires publics ou privés.

1 Article

2 Electronically Re-Configurable Non-Volatile 3 Nano-Ionics based RF-Switch on Paper Substrate for 4 Chipless RFID Applications

5 Jayakrishnan M.P. ^{(1,*), Arnaud Vena ^{(2), Brice Sorli ^{(2) and Etienne Perret ^(1,3)}}}

6 ¹ Univ. Grenoble Alpes, Grenoble INP, LCIS, 26902 Valence, France.

7 Email: jayakrishnan.mp@lcis.grenoble-inp.fr, etienne.perret@lcis.grenoble-inp.fr

8 ² Institut d'Electronique et Systèmes (IES), Université de Montpellier 2, Montpellier 34095, France.

9 Email: arnaud.vena@umontpellier.fr, brice.sorli@ies.univ-montp2.fr

10 ³ Institut Universitaire de France, 75005 Paris, France.

11 * Correspondence: jayakrishnan.mp@lcis.grenoble-inp.fr

12 Received: date; Accepted: date; Published: date

13 **Abstract:** This article reports the first results of a Nafion® based solid state Non-Volatile
14 electronically reconfigurable RF-Switch integrated to a Co-Planar Waveguide transmission line
15 (CPW) in shunt mode, on flexible paper substrate. The switch is based on a Metal-Insulator-Metal
16 structure formed respectively using Silver-Nafion-Aluminum switching layers. The presented
17 device is fully passive and shows good performance till 3GHz, with an insertion loss less than 3dB
18 in the RF-On state and isolation greater than 15dB in the RF-Off state. Low power DC pulses in the
19 range 10V/0.5mA and -20V/0.15A are used to operate the switch. The device is fabricated in an
20 ambient laboratory condition, without the use of any clean room facilities. A brief discussion on the
21 results and a potential application of this concept in a re-configurable chipless RFID tag is also
22 given in this article. This study is a proof of concept, of fabrication of electronically Re-Configurable
23 and disposable RF electronic switches on low cost and flexible substrates, using a process feasible
24 for mass production.

25 **Keywords:** CBRAM, MIM Switch, Chipless RFID, RF-Switch, Reconfigurable Switch
26

27 1. Introduction

28 Low-power, Passive and Non-Volatile RF-switches are an area of keen interest among the
29 scientists and industry in the current decade. Non-volatile switches would benefit every field of
30 RF-engineering by drastically cutting down the power budget. With the current threshold of
31 development in disposable printed RF electronics, the requirement for passive and low power
32 switches has been intensified.

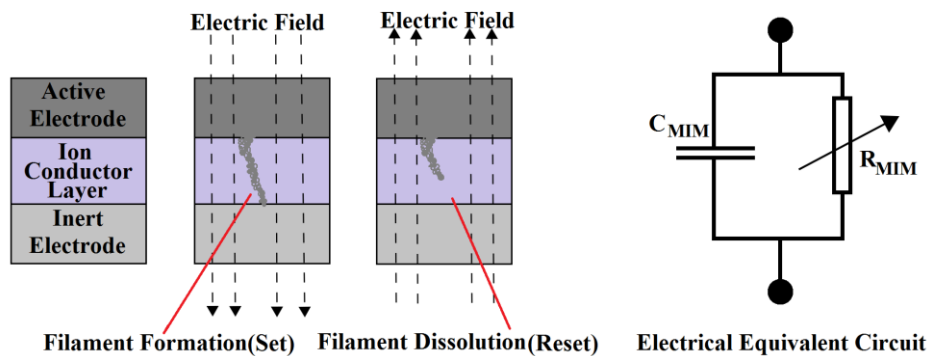
33 One of the available solution for Passive non-volatile switches are the Memristive devices such
34 as the Conductive Bridging Random Access Memory (CBRAM) switches [1], Phase Change Memory
35 (PCM) switches [2,3] etc. These techniques utilize electrochemical properties and molecular
36 arrangement properties of materials respectively to achieve the switching action. The CBRAM
37 switch is also referred to as a Metal-Insulator-Metal (MIM) switch owing to its switching layers
38 construction. Working principle and details of this technology is explained in this article. In case of
39 the PCM switches, the change from amorphous to crystalline state and back, of certain materials like
40 Germanium Telluride upon application of controlled heating pulses are utilized for switching. A
41 handful of articles have reported fine non-volatile switches based on the above mentioned
42 principles[1,2,4–6]. However, in majority cases, the fabrication technique is very much complicated
43 and often requires a 'clean room' facility for the same. And in most cases the devices are fragile in
44 nature and require dedicated conformal protection schemes to protect it from the ambient
45 atmosphere and thus adds to the total cost budget.

46 In this article for the first time we present the design, development and application of a simple
 47 and robust CBRAM based MIM RF-switch on flexible paper substrate. In this experiment, the entire
 48 device fabrication was carried out in ambient laboratory conditions, without the use of any clean
 49 room facilities. In this study, we aim to prove the feasibility of integrating a MIM switch in
 50 electronically reconfigurable RF devices on flexible and low cost substrates like paper, which are
 51 seen around in our daily life as packaging materials for goods, transport tickets and visiting cards.

52 An RF-Identification tag using the RF-Encoding particle proposed in this paper could be easily
 53 fabricated as a sticker, on a paper substrate with adhesive background and could be attached to an
 54 object, like a barcode sticker, with far more advanced functionalities in comparison to the optical
 55 barcodes, like identification out of the optical-line-of-sight, electronic reconfigurability etc.

56 2. Motivation and Background

57 The basic building block of the presented RF-Switch is a nano-ionic MIM switching cell. Fig. 1
 58 shows the basic layer structure and working principle of the proposed switching technique. The
 59 MIM cell is comparable to a parallel plate capacitor in which the electrolyte is replaced by an
 60 ion-conductor, which is an electrically insulating material, such as PMMA[7] or doped Chalcogenide
 61 glass [4], or Nafion [8], etc. One electrode of the cell is an ion-donor metal like silver or copper,
 62 generally called the active electrode and the other is a relatively inert metal like aluminum or gold.
 63 On the application of an electric field from active to inert electrode, ions from active electrode under
 64 the influence of this field grow a filament to inert electrode, through the ion-conductor layer. This
 65 closes the switch, to form the Set state, with a low resistance across the cell. Similarly, a field of
 66 opposite direction is used to dissolve the filament and open the switch to form the Reset state, with a
 67 high resistance across the cell. The switch once commuted to a stable state does not require any
 68 maintaining power supply to retain its state, making it a non-volatile passive device. Power is
 69 applied to the switch only to change its state. Electrical equivalent model of the MIM switch could be
 70 approximated to a parallel plate capacitor in parallel to the filament resistance as shown in Fig. 1,
 71 where C_{MIM} is equivalent capacitance due to geometry of electrodes and R_{MIM} is equivalent filament
 72 resistance across the cell.



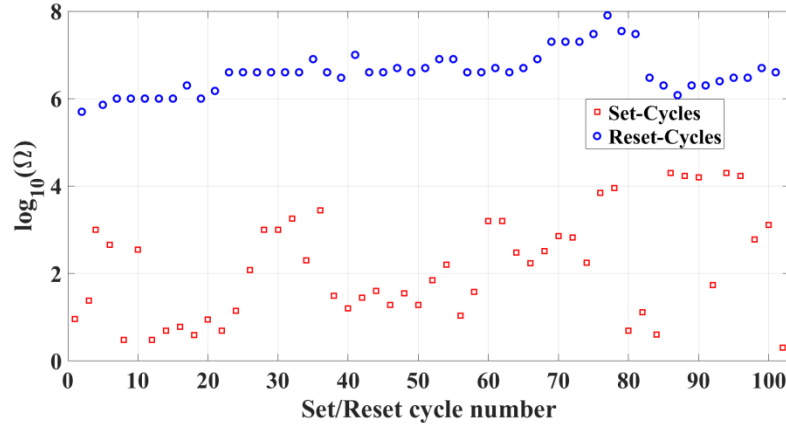
73 **Fig. 1** Layer architecture of MIM cell showing the filament formation and dissolution, along with the
 74 electrical equivalent circuit.

75 The Fig. 2 shows 100 switching cycles for a typical MIM cell with Nafion as ion-conductor v/s
 76 filament resistance. We have not yet done a full-fledged study to find out the maximum number of
 77 functional cycles or the switching time of the MIM cell, to preserve the devices for detailed
 78 RF-characteristics analysis. This would be carried out in near future.

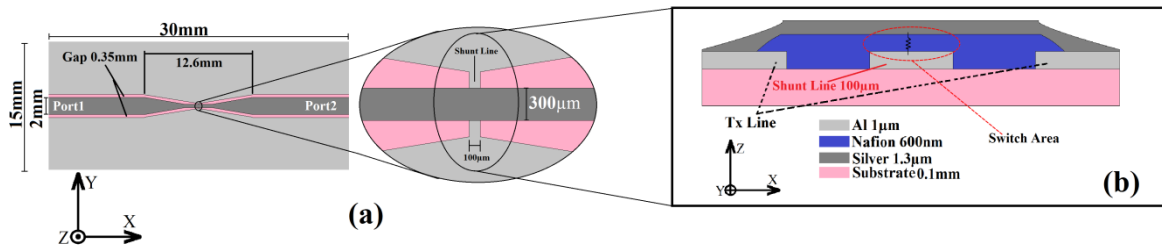
79 3. Design and Construction

80 The presented design is a modified version of the predecessor reported in [8]. The reported
 81 version in this article [8] is a 50Ω CPW switch in shunt mode on FR-4 substrate, similar to the one
 82 shown in Fig. 3. This device is fully fabricated in an ambient environment without the use of any
 83 clean room facilities. The device shows good performance features at least up to 3GHz in

84 comparison with existing switching technologies available. The CPW shunt mode design is chosen
 85 over the simple Microstrip design to avoid the fabrication difficulties in ambient laboratory
 86 conditions. With the Microstrip design, there are size limitations on the dimensions of the switching
 87 area in order to limit very high capacitance at higher frequencies. This requires having very small
 88 dimensions than what is used in this study. The photograph of this realization is depicted in Fig 4 (a)
 89 and the inset shows the close-up microphotograph of the MIM switch area.



90 **Fig. 2** 100 switching cycles of a typical MIM cell with Nafion as the ion-conductor.



91 **Fig. 3** Geometry (a), and layer architecture (b) used in the CPW shunt mode RF-Switch

92 In this article we try the same technology on flexible paper substrate. The topology and
 93 dimensions of the switch are given in Fig. 3. Process used for the fabrication is detailed in the
 94 following paragraphs.

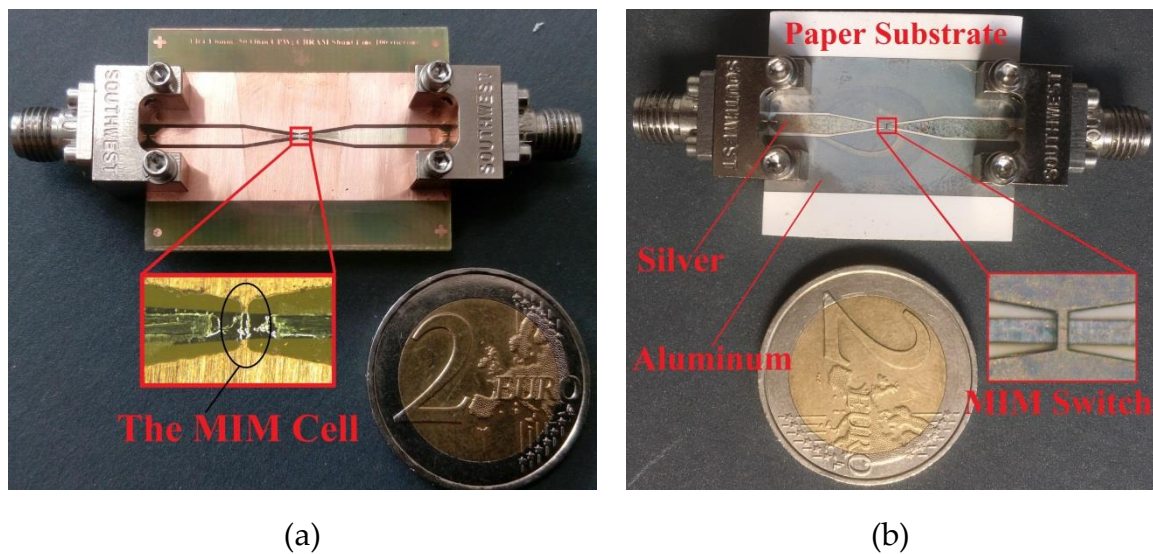
95 The substrate used for the fabrication of the device is 80 grams per sq. meter (GSM) special
 96 quality RF-paper developed at the IES lab. This paper is flexible and specially treated to reduce the
 97 losses at radiofrequencies and also has an improved surface for better adhesion of metal layers.
 98 Metal layers are formed on the substrate by thermal vapor deposition of Silver (Active electrode)
 99 and Aluminum (Inert electrode). Thermal vapor deposition is done with the help of dedicated
 100 Nickel masks which carry an engraved aperture of the presented topology in Fig. 3. After formation
 101 of the active electrode, the electrolyte layer is formed by spin coating the Nafion solution (supplied
 102 by Sigma Aldrich) at a rate of 500RPM for 30 seconds. The formed layer is then air dried on a hot
 103 plate at 100°C for 2 min. Then the inert electrode is formed using thermal vapor deposition.
 104 Detachable SMA connectors are then attached to the device to feed RF power.

105 It is now apparent that the proposed switch could be integrated into most RF- Designs using a
 106 three step process. 1. Deposition of active electrode. 2. Deposition of electrolyte/ion-conductor. 3.
 107 Inert electrode deposition. These steps could be easily carried out in an industrial environment by
 108 techniques like flexography[9]. The use of silver metal in the tags could be limited to the switch area
 109 only, by adjusting the nickel mask design, so as to reduce further the cost of realization.

110 Photograph of the fabricated CPW shunt mode switch is shown in Fig. 4 (b) and the inset shows
 111 the microphotograph of MIM switch area revealing the sandwich structure. The thickness of Silver
 112 and Aluminum deposit is measured to be 1.3μm and 1μm respectively and that of Nafion deposit is
 113 600nm. The measurement is carried out with the help of Dektak-150 mechanical Profilometer.

114 Nafion [8] is chosen as the ion-conductor in this realization due to some specific advantages
115 inherent to this polymer in contemplation to materials used classically [4]. Nafion is a sulfonated
116 tetrafluoroethylene based fluoropolymer-copolymer, well known for its fast ion conducting
117 properties and use in proton-exchange-membrane fuel cells, and is stable upto 190°C [10]. Nafion
118 layer could be easily formed by spin coating and could be air-dried at temperatures around 100°C.
119 From our experience in realization, this material is stable in the ambient air and do not require an
120 additional conformal coating for protection. The maximum temperature observed on the sample
121 during the thermal vapor deposition in around 120°C.

122 Working of the presented CPW shunt mode switch could be explained with reference to Fig. 3.
123 MIM switch structure is formed in this device between the 100 μm wide shunt line and 300 μm wide
124 transmission line sandwiching 600nm layer of Nafion. Shunt line connects the two ground planes on
125 either side of the CPW line. When the MIM switch is Set as shown in Fig. 1, at the switch area labeled
126 in Fig. 3 (b), RF power from Port 1 is short circuited to ground, thus disconnecting it from Port 2.
127 This is the RF-Off state of the switch. When the MIM switch is Reset as shown in Fig. 1, the short is
128 removed and Port 1 is connected to Port 2, forming the RF-On state.



129 **Fig. 4** Photographs of the fabricated RF-Switch on classic FR-4 substrate (a), and on paper substrate
130 (b). Inset of both photographs shows the microphotograph of the MIM switch area.

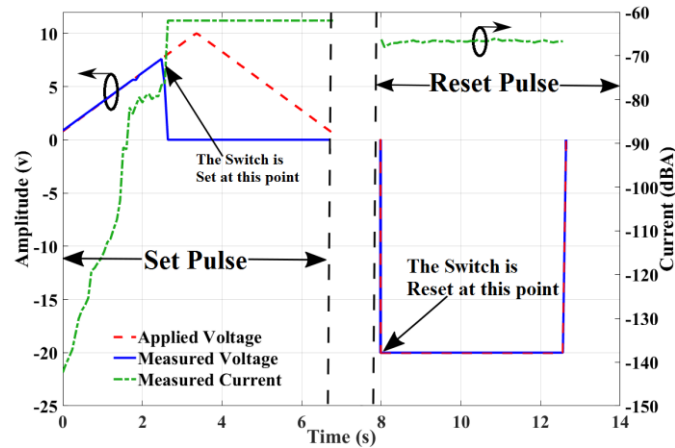
131 DC pulses used for operating the switch are given in Fig. 5. In order to ensure smooth and
132 stable operation of the switch, a positive growing current limited triangular wave form of peak
133 voltage 10V/0.5mA is used for the Set and a flat -20V/0.15A square wave is used for the Reset as
134 shown in the plot. These wave forms are optimized by various trial and error experiments. In the
135 case given in Fig. 5, switch is Set at 7.5V and Reset at -20V, power consumed for the Set and Reset are
136 calculated as 0.76mW and 9.6mW respectively. These power values are calculated from the
137 instantaneous value of Set/Reset voltage and current pulses. An abrupt fall in the measured voltage
138 across the switch and rise in current during the Set pulse indicates a Set state by the formation of a
139 low resistance filament from active to inert electrode in the MIM Cell (see Fig. 5). Similarly an abrupt
140 rise in voltage and fall in current during the Reset pulse indicates dissolution of filament and
141 establishment of high resistance Reset state across the MIM cell. The Set/Reset pulses were applied
142 to the switch with the help of custom made metallic probes attached to metallic parts of the switch.

143 **4 Results**

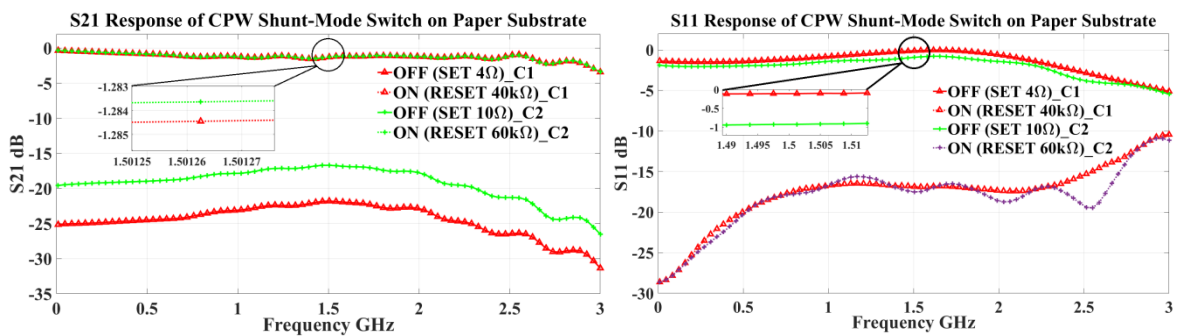
144 RF response of the switch is given in Fig. 6. Measurements of the device is done using Agilent
145 ENA E5061B (3GHz) Network Analyzer, using Short-Open-Load-Thru calibration scheme. Power
146 level used for the test is -15dBm. The RF-switch shows acceptable performance up to 3GHz with an
147 insertion loss less than 3dB in RF-On condition and isolation greater than 15dB in the entire band, in

148 RF-Off condition. Filament resistance values for the respective Set and Reset are given in brackets of
 149 the respective legends for each cycle of operation. We were able to achieve filament resistance values
 150 of 4Ω and $60k\Omega$ respectively for Set and Reset states.

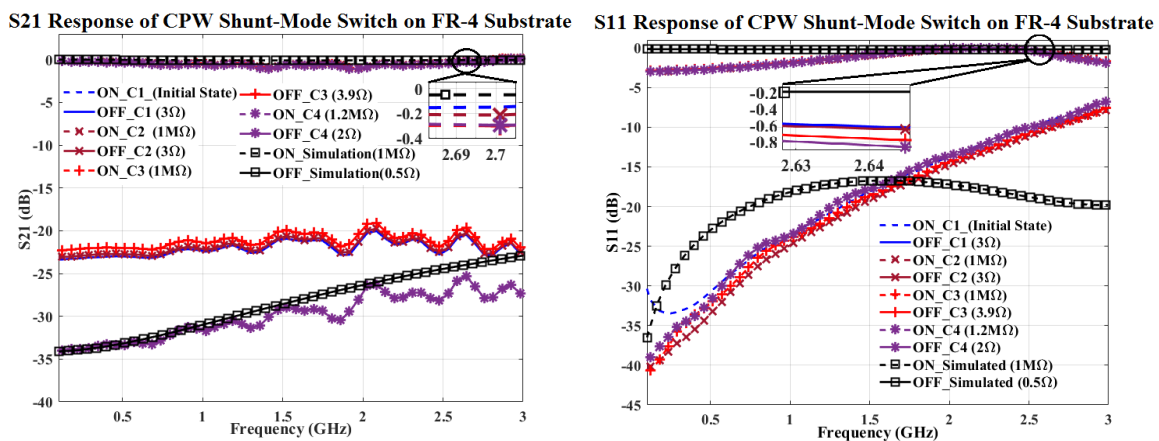
151 In this experiment the maximum Set resistance value is 10Ω and the minimum Reset resistance
 152 value is $40k\Omega$. This is a good R_{Reset}/R_{Set} value. RF response of realization of the CPW shunt mode
 153 switch on classical FR-4 substrate [8] is given in Fig. 7 for comparison. This device shows an insertion
 154 loss less than 1dB in RF-On state and greater than 16dB in the RF OFF state. From this response it is
 155 clear that the realization on paper substrate has acceptable performance. Minor degradation in the
 156 On-state insertion loss could be justified by the losses inherent to paper substrate.
 157



158 Fig. 5 DC pulses used to operate the switch.



159 Fig. 6 RF-Response of the CPW shunt mode switch, on paper substrate.



160 Fig. 7 RF-Response of the CPW shunt mode switch, on FR-4 substrate.

161 Table 1. is a comparison of the features of proposed RF-Switch on paper substrate with the
 162 state of the art and design on classic FR-4 substrate.

163 Table1. Comparison of proposed device to state of the art.

Features	Proposed design on paper substrate	Design on FR4 [8]	State of the Art (Nano-Ionic Switch) [4]
Min. Fabrication size Requirement	100 μ m	100 μ m	10 μ m
Frequency Range	DC - 3GHz	DC - 3GHz	DC - 6GHz
Isolation (avg.) (Off state)	-23dB	-16dB to -34dB	-35dB
Insertion Loss(avg.) (On state)	1.2dB	0.5dB	0.5dB
Actuation Voltage	~10V/-20V*	~10V/-20V*	~1V
Power Consumption	μ W/mW*	μ W/mW*	μ W
Energy Consumption to Maintain State	0	0	0
'Set' - Resistance (avg.)	7 Ω	2-5 Ω	10 Ω
Switching Speed	#	#	1 - 10 μ s
Alignment Accuracy required for fabrication	Low	Low	Very High
Number of Fabrication Steps	3	6	6 (Clean Room Procedures)
Fabrication Environment	Ambient room	Ambient room	Clean room
Fabrication Cost (Laboratory Perspective)	Low	Low	High
Fabrication Cost (Industrial Perspective)	Low	Low	Moderate

164 * For Set/Reset respectively. # At present, we do not have enough information for calculating the switching time
 165 of the presented device.

166 5. Potential Applications

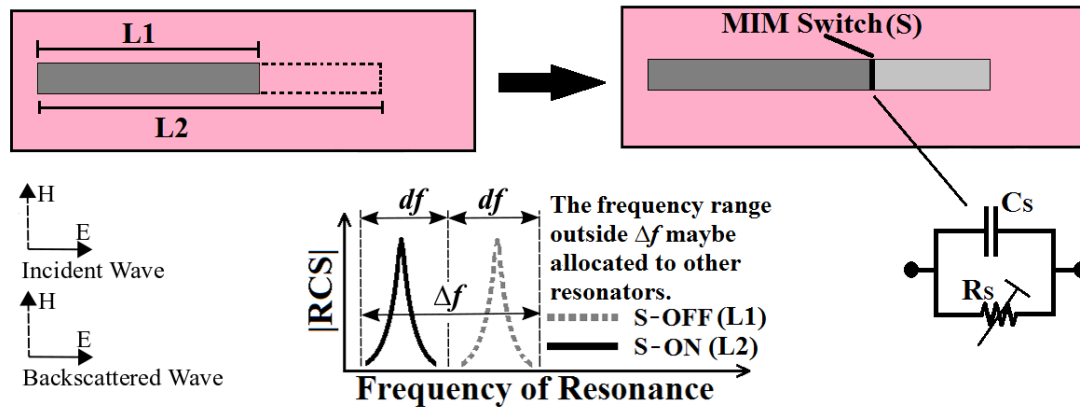
167 This idea of fabrication of RF-switches is seen to be functional and feasible in several
 168 applications in the field of disposable RF-Electronics, in devices such as reconfigurable RFID Tags
 169 [11,12], reconfigurable filters and reconfigurable antennas.

170 Radio Frequency Identification or RFID is a multi-dimensional ingenious concept that has
 171 evolved in the past couple of decades and still advancing at a very high speed. RFID finds
 172 application in an all-round domain from identification, sensing, energy harvesting etc. [12-14]

173 Amongst this, the chipless-RFID technology is an innovative identification technique often referred
 174 to as the 'Barcode of the future' due to its various versatile functionalities like large read range
 175 without optical contact, sensor integration functionality [11,14,15] etc., which cannot be
 176 implemented in the current scenario, with the optical barcode technology. Still a limiting factor to
 177 widespread use of this technology is the cost per unit tag in comparison to optical barcodes.
 178 However, recent developments in the field of disposable printed RF-electronics would lift this
 179 technique, to the technology main stream in near future. Thanks to CBRAM switches for adding
 180 revolutionary reconfigurability functionality to the chipless RFID tags, which would help in
 181 reducing cost per unit tag and increase the versatility of this technique.

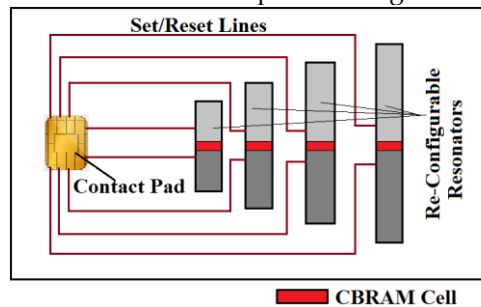
182 An example of potential advantage of using the proposed switch technology could be explained
 183 as follows. Fig. 8 shows the method of frequency shift coding of RF-Encoding Particles (REP) in a
 184 chipless RFID tag [10,14]. In this example a shorted dipole resonator is used as the REP. Classically,

185 this is achieved by modifying the dimensions of each REP on the tag as shown in Fig. 8, for this, a
 186 unique geometry has to be designed for each REP. But instead, if we introduce the proposed MIM
 187 switch technique to this REP as shown in Fig. 8, the same performance could be achieved with a
 188 general REP of fixed dimension, by electronically switching the MIM cell.



189 **Fig. 8** Concept of application of MIM switches in an REP for chipless RFID tag.

190 If we integrate such REPs depending on how much bit density is required, on a credit card size
 191 tag, with contact pad and Set/Reset lines, it forms a general reconfigurable chipless RFID Card. This
 192 could be programmed by a dedicated logic device similar to a credit card reader to encode
 193 information. And then could be used for identification in wireless mode similar to a conventional
 194 chipless RFID tag. An illustration of this idea is depicted in Fig. 9.



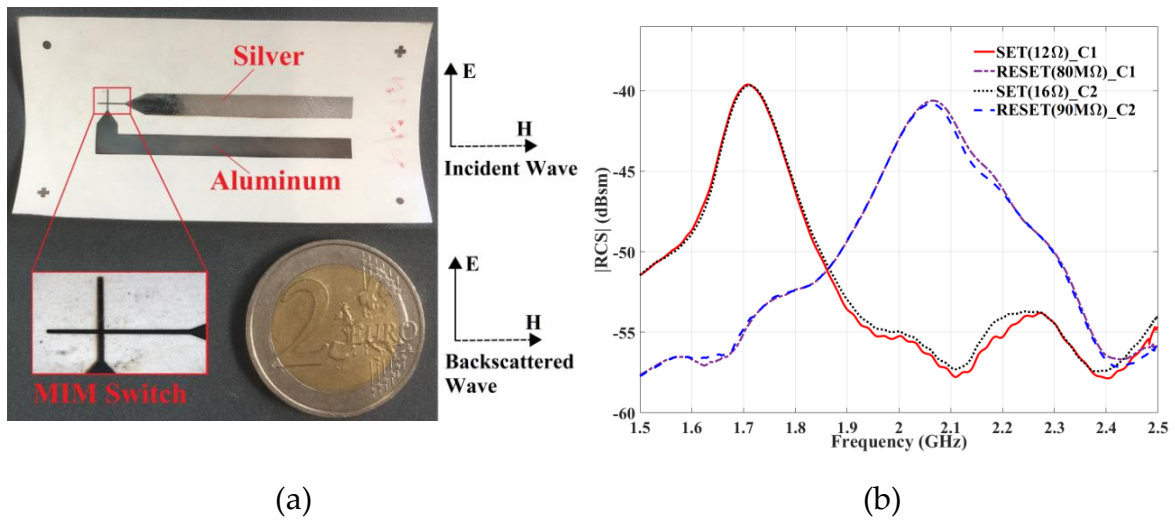
195 **Fig. 9** Conceptual illustration of an electronically reconfigurable chipless RFID tag.

196 The proof of concept of this technique is reported in [10], and Fig. 10 (a) and (b) shows
 197 respectively the photograph and response of a similar design on flexible paper substrate. Fabrication
 198 of this tag is carried out in similar way like the RF switch on paper, by thermal vapor deposition of
 199 Silver (active) and Aluminum (inert) electrodes, and spin coating of Nafion. The proposed design is
 200 inspired from the 'C' resonator reported in [16]. Here we use a MIM switch, as shown in Fig.10 (a)
 201 with Silver-Nafion-Aluminum layers, to reconfigure the resonator by tuning its electrical equivalent
 202 circuit depending on the filament resistance (of the nano-ionic filament in the MIM cell). Equivalent
 203 circuit analysis and simulation studies of this concept are reported in [10]. Fig. 11 shows the
 204 experimental Bistatic Radar setup using Agilent N5222A PNA and two wide band horn antennas in
 205 co-polarization in an anechoic chamber [16]. This setup is used to record the RCS response of the tag
 206 shown in Fig.10. It is apparent from these results that we are able to switch the tag at two different
 207 resonant frequencies separated by 400MHz, with Set/Reset position of the MIM switch.

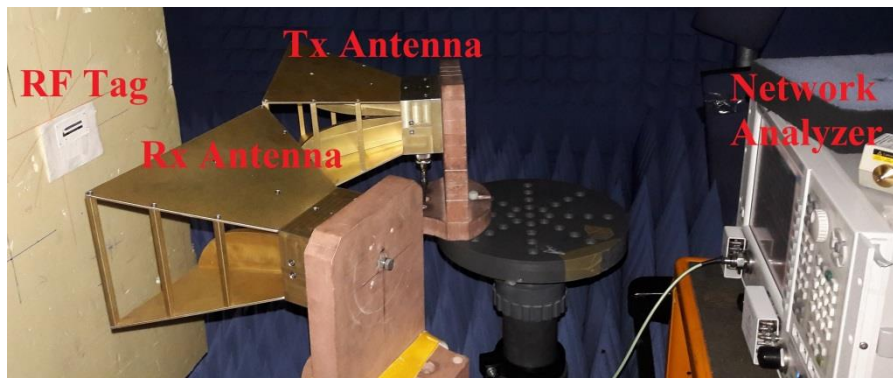
208 Discussion on the application of this concept for a commercial mass production and use, and
 209 the expected convenience is explained in the following paragraphs.

210 [17] Reports a 20-bit chipless RFID tag. Let's suppose to use this particular tag for labeling
 211 application in which the tag is encoded by using two different dimensions for each resonator. Thus
 212 by using the well-known frequency shift coding technique [14] expression (1) could be used to
 213 compute the possible number of combinations (refer Fig. 8 for illustration of the concept of
 214 bandwidth allocation for each resonator).

$$N = \left[\frac{\Delta f}{df} \right]^k \quad (1)$$



215 **Fig. 10** Photograph (a) and measured $|RCS|$ response (b) of the reconfigurable RF-tag on paper
 216 substrate.



217 **Fig. 11** Bistatic Radar setup used for RCS measurements of the Tag.

218 In (1) Δf is the allocated bandwidth per resonator, df is the bandwidth of resonance of the
 219 resonator, k is the number of resonators on the tag, and N is the total number of possible
 220 combinations. In this example let us say the allocated bandwidth per resonator is 200MHz and each
 221 resonator resonates with a bandwidth of 100MHz. So each resonator could be reconfigured by
 222 modifying physical size to operate in two different frequencies in the allocated bandwidth. Thus
 223 using (1) we could see that the total number of possible combinations is 1048576. Now if we try to
 224 fabricate the required combinations of tags using classical techniques like screen printing or
 225 photolithography, one requires 1048576 numbers of masks for the realization of the entire stretch of
 226 tags.

227 Beauty of the proposed concept could be revealed in the following sentences, taking into
 228 consideration the amount of labor and number of masks required for the fabrication. If a MIM switch
 229 is introduced to each resonator as in [10], to switch resonators between two different frequencies. It
 230 is apparent from the presented work that the switch/tag could be fabricated using just two masks
 231 and spin coating of Nafion. Similarly, for this particular RFID tag, the entire stretch of tags could be
 232 fabricated as a general tag using just two masks. Then, a dedicated electronic pulse programming
 233 circuit with an electrode array could be used to Set/Reset the respective switches and to encode each
 234 tag. In essence, the complexity of requirement of 1048576 unique masks for fabrication is solved by

235 just using two masks and a dedicated programmer circuit. This example clearly indicates the
236 leverage of application of this technology in reconfigurable chipless RFID tags.

237 6. Conclusion

238 In this article, we have presented the design, construction and response of CPW shunt mode
239 switch on flexible paper substrate. The speciality of this application is the simplicity in fabrication of
240 the device on a substrate available at a very low cost, without using any clean room facilities. The
241 operation of the switch is tested for at least 50 cycles for several batches, and the results are
242 repeatable and reproducible respectively. We have also explained and proved the concept of
243 integration of CBRAM or MIM switch technology in chipless RFID tags which are fabricated using
244 simple steps on low cost paper substrates. The outcomes of this experiments show a promising bright
245 future for this technique. Reconfigurable chipless RFID could be the potential labels of tomorrow,
246 backing the idea of Internet-of-Things[11,15]. This switch technique could also be applied in devices
247 like reconfigurable filters and reconfigurable antennas in similar way, which are in development
248 with the authors. With these results and the imparted confidence, the authors of this article are very
249 near to the realization of fully printed electronically reconfigurable RF-Switches and chipless RFID
250 tags on paper, using electrolyte solvents and conductive inks, using an inkjet printer.

251 **Author Contributions:** Conceptualization, Jayakrishnan M.P., Arnaud Vena and Etienne Perret;
252 Methodology, Jayakrishnan M.P.; Software, Jayakrishnan M.P., Arnaud Vena and Etienne Perret; Validation,
253 Jayakrishnan M.P., Arnaud Vena, Brice Sorli and Etienne Perret; Writing-Original Draft Preparation,
254 Jayakrishnan M.P.; Writing-Review & Editing, Jayakrishnan M.P., Arnaud Vena and Etienne Perret;
255 Supervision, Arnaud Vena, Brice Sorli and Etienne Perret; Project Administration, Arnaud Vena, Brice Sorli
256 and Etienne Perret; Funding Acquisition, Brice Sorli and Etienne Perret

257 **Funding:** This research is funded and supported by the Grenoble Institute of Technology, Université Grenoble
258 Alpes, France and Institut Universitaire de France.

259 **Acknowledgments:** The authors are grateful to the Institut d'Electronique et Systèmes (IES) University of
260 Montpellier 2, France, for supporting this project

261 **Conflicts of Interest:** The authors declare no conflict of interest

262 References

- 263 1. Michael N. Kozicki; William C. West Programmable metallization cell structure and method of making
264 same 1998.
- 265 2. Wang, M.; Shim, Y.; Rais-Zadeh, M. A Low-Loss Directly Heated Two-Port RF Phase Change Switch.
266 *IEEE Electron Device Letters* **2014**, *35*, 491–493, doi:10.1109/LED.2014.2303972.
- 267 3. Mahanta, P.; Munna, M.; Coutu, R. A. Performance Comparison of Phase Change Materials and
268 Metal-Insulator Transition Materials for Direct Current and Radio Frequency Switching Applications.
269 *Technologies* **2018**, *6*, 48, doi:10.3390/technologies6020048.
- 270 4. James Nessel; Richard Lee Chalcogenide nanoionic-based radio frequency switch 2011.
- 271 5. Pi, S.; Ghadiri-Sadrabadi, M.; Bardin, J. C.; Xia, Q. Nanoscale memristive radiofrequency switches. *Nature*
272 *Communications* **2015**, *6*, 7519, doi:10.1038/ncomms8519.
- 273 6. El-Hinnawy, N.; Borodulin, P.; Wagner, B. P.; King, M. R.; Jones, E. B.; Howell, R. S.; Lee, M. J.; Young, R.
274 M. Low-loss latching microwave switch using thermally pulsed non-volatile chalcogenide phase change
275 materials. *Appl. Phys. Lett.* **2014**, *105*, 013501, doi:10.1063/1.4885388.
- 276 7. Perret, E.; Vidal, T. L.; Vena, A.; Gonon, P. Realization of a Conductive Bridging RF Switch Integrated
277 onto Printed Circuit Board. *Progress In Electromagnetics Research* **2015**, *151*, 9–16,
278 doi:10.2528/PIER14120403.

- 279 8. Jayakrishnan, M. P.; Vena, A.; Meghit, A.; Sorli, B.; Perret, E. Nafion-Based Fully Passive Solid-State
280 Conductive Bridging RF Switch. *IEEE Microwave and Wireless Components Letters* **2017**, *27*, 1104–1106,
281 doi:10.1109/LMWC.2017.2764741.
- 282 9. Heitner-Wirguin, C. Recent advances in perfluorinated ionomer membranes: structure, properties and
283 applications. *Journal of Membrane Science* **1996**, *120*, 1–33, doi:10.1016/0376-7388(96)00155-X.
- 284 10. Jayakrishnan, M. P.; Vena, A.; Sorli, B.; Perret, E. Solid-State Conductive-Bridging Reconfigurable
285 RF-Encoding Particle for Chipless RFID Applications. *IEEE Microwave and Wireless Components Letters*
286 **2018**, *28*, 506–508, doi:10.1109/LMWC.2018.2830702.
- 287 11. Etienne Perret *Radio Frequency Identification and Sensors: From RFID to Chipless RFID*; Wiley: Hoboken, NJ,
288 USA, 2014; ISBN 978-1-84821-766-9.
- 289 12. Lemey, S.; Agneessens, S.; Van Torre, P.; Baes, K.; Vanfleteren, J.; Rogier, H. Wearable Flexible
290 Lightweight Modular RFID Tag With Integrated Energy Harvester. *IEEE Transactions on Microwave Theory*
291 *and Techniques* **2016**, *64*, 2304–2314, doi:10.1109/TMTT.2016.2573274.
- 292 13. Goncalves, R.; Rima, S.; Magueta, R.; Pinho, P.; Collado, A.; Georgiadis, A.; Hester, J.; Carvalho, N. B.
293 RFID-Based Wireless Passive Sensors Utilizing Cork Materials. *IEEE Sensors Journal* **2015**, *15*, 7242–7251,
294 doi:10.1109/JSEN.2015.2472980.
- 295 14. Arnaud Vena; Etienne Perret; Smail Tedjini *Chipless RFID based on RF Encoding Particle: Realization, Coding*
296 *and Reading System*; ISTE-Elsevier: New York, NY, USA; ISBN 978-1-78548-107-9.
- 297 15. Tedjini, S.; Karmakar, N.; Perret, E.; Vena, A.; Koswatta, R.; E-Azim, R. Hold the Chips: Chipless
298 Technology, an Alternative Technique for RFID. *IEEE Microwave Magazine* **2013**, *14*, 56–65,
299 doi:10.1109/MMM.2013.2259393.
- 300 16. Vena, A.; Perret, E.; Tedjini, S. Chipless RFID Tag Using Hybrid Coding Technique. *IEEE Transactions on*
301 *Microwave Theory and Techniques* **2011**, *59*, 3356–3364, doi:10.1109/TMTT.2011.2171001.
- 302 17. Vena, A.; Perret, E.; Tedjini, S. A Fully Printable Chipless RFID Tag With Detuning Correction Technique.
303 *IEEE Microwave and Wireless Components Letters* **2012**, *22*, 209–211, doi:10.1109/LMWC.2012.2188785.
- 304



307 © 2018 by the authors. Submitted for possible open access publication under the
terms and conditions of the Creative Commons Attribution (CC BY) license
(<http://creativecommons.org/licenses/by/4.0/>).